28th ABCM International Congress of Mechanical Engineering
November 09-14, 2025, Curitiba-PR, Brazil

COB-2025-0446
Numerical Analysis of Surface Walls for Ground Vibration Attenuation Using the Perfectly Matched Layer Method

Isadora Rodrigues de Souza
Jenario Souza dos Reis
Simone dos Santos Hoefel
Federal University of Piauí, Campus Universitário Ministro Petrônio Portella - Ininga, 64049-550, Teresina PI, Brazil
jenariojunior4@gmail.com, irs08902@gmail.com, simone.santos@ufpi.edu.br

Amanda Morais de Oliveira
Josué Labaki
School of Mechanical Engineering, University of Campinas, R. Mendeleyev, 200, 13083-860, SP, Brazil
a261912@dac.unicamp.br, labaki@unicamp.br

Abstract. *The dynamic response of structures interacting with the soil is a topic of significant interest, as vibrations propagating through the soil can compromise the performance and safety of vibration-sensitive facilities. The damaging effects of ground-borne vibration can be mitigated with the installation of surface walls, provided adequate geometric and constitutive properties are selected for the walls. The effect of constitutive and geometric parameters of surface walls in their vibration attenuation performance can be analyzed using various numerical techniques. This work presents an analysis of the vibration attenuation performance of surface walls using the Perfectly Matched Layer (PML) method. The PML method, widely used in fields such as electromagnetism, acoustics, and elastodynamics, uses a complex coordinate stretching formulation of energy-absorbing layers that can be incorporated into the boundaries of finite domains. These layers effectively absorb incident waves at any angle and frequency, thereby minimizing reflections at the model boundaries. The incorporation of these energy-absorbing layers causes finite domains to behave as unbounded domains, in the sense that they comply with Sommerfeld's radiation condition. Hence, the PML is an effective way to obtain an accurate representation of unbounded domains, like the soil, while using classical finite domain discretizations. This method is used in this paper to model the response of various configurations of surface walls interacting with the soil. Numerical results show excellent agreement with reference solutions, confirming the accuracy of the PML modeling. Additional simulations are performed to assess the influence of depth of wall embedment on ground vibration attenuation. The results demonstrate that partially buried walls enhance isolation performance and that increasing the depth of embedment shifts the insertion loss peak toward higher frequencies. The proposed formulation provides a reliable framework for analyzing dynamic soil–structure interaction problems involving vibration mitigation using embedded or surface structures.*

Keywords: *Vibration Attenuation, Soil Structure Interaction, Perfectly Matched Layer Method, Surface Walls*

1. INTRODUCTION

Ground vibrations induced by traffic loads, construction blasting, heavy machinery, or natural sources such as earthquakes not only affect sensitive equipment and damage structures, but also disrupt residents' daily lives. As a result, studying vibration attenuation techniques is essential.

Common types of vibration isolation barriers include trenches (Pu *et al.*, 2018), piles (Jiang *et al.*, 2020), periodic structures (Li *et al.*, 2023)and surface walls (Carneiro *et al.*, 2022). Continuous barriers, such as open or filled trenches, are widely used due to their cost-effectiveness and good vibration attenuation performance. However, their application is limited by the need for deep excavations, which may compromise trench stability. Moghadam and Rafiee-Dehkharghani (2022) compared the performance of open and filled trenches in single-phase and saturated soils, concluding that barriers are more effective in saturated conditions.

Discontinuous barriers, such as piles, offer a viable alternative, particularly due to their ability to be driven to great depths and arranged in various configurations to block wave propagation. Several studies have investigated their effectiveness in mitigating ground vibrations through numerical modeling. Barros *et al.* (2019) proposed a numerical model for the time-harmonic vertical response of a system consisting of a rigid circular plate on the ground surface and an embedded pile, showing that short piles have negligible impact on the system's static impedance. Using a three-dimensional boundary element method in the frequency domain, Tsai *et al.* (2008) analyzed the vibration reduction performance of four types of piles and concluded that pile length has a greater influence on screening effectiveness than pile spacing or the distance between the vibrating foundation and the pile barrier.

The use of heavy masses on the ground surface can be considered a better alternative to traditional mitigation measures, due to simpler implementation and lower construction and maintenance costs (Baziar and Shahbazan, 2024). Using a coupled 2.5D numerical approach combining finite and boundary elements, Dijckmans *et al.* (2015) showed that continuous gabions or concrete walls on the surface can be modeled as mass-spring systems, significantly reducing vibration levels at frequencies just above the system's resonance. Carneiro *et al.* (2022) demonstrated that for surface walls narrower than the incident wavelength, maximum mitigation level occurs at the resonance frequencies of the mass-spring system and increasing the width of the blocks does not necessarily affect their vibration attenuation performance positively.

This work investigates the effectiveness of partially buried walls in attenuating time-harmonic vibrations. The Perfectly Matched Layer (PML) technique in used to model wave propagation in elastic media involving surface and partially buried structures. The soil and structural components are modeled as two-dimensional, linear, isotropic, and elastic materials, and discretized using the Finite Element Method (FEM). The PML is implemented through a complex coordinate transformation to minimize reflections at the boundaries of the computational domain. Model validation is conducted by reproducing benchmark cases from the literature, including surface plates, piled plates, and surface walls.

1.1 Problem statement

The problem consists of a wall that is partially buried in the soil, illustrated in Fig. 1. The computational domain is defined as a two-dimensional rectangular region with width W and height H, representing an elastic half-space. A single vertical wall with width L and total height H is placed at the surface, partially embedded into the soil to a depth H_s. A harmonic vertical excitation of amplitude F and angular frequency ω, given by $Fe^{i\omega t}$, is applied at point A, located at a horizontal distance d from the center of the wall. The system response is evaluated at point B, positioned at the soil–structure interface. To simulate an unbounded domain and avoid wave reflections at the boundaries, Perfectly Matched Layers (PML) with thickness T_{PML} are added along the lateral and bottom edges of the computational domain. Both the soil and the wall are considered homogeneous, isotropic, and linear elastic materials, characterized by their respective Young's modulus E, Poisson's ratio ν, and mass density ρ.

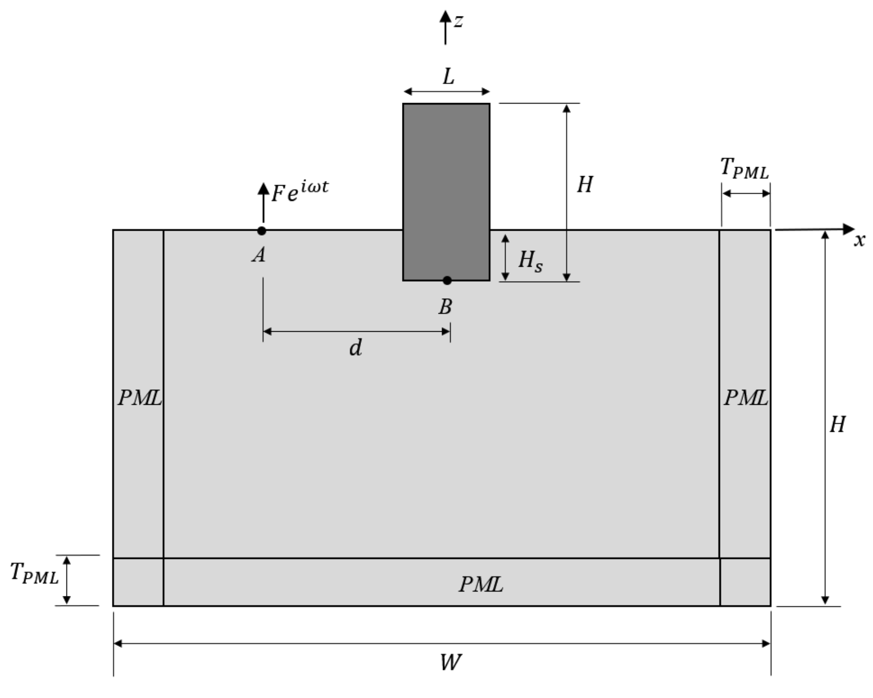

Figure 1: Partially buried wall and soil domain considered.

2. FORMULATION

2.1 Finite Element Method (FEM)

The soil and structural components in this paper are modeled as two-dimensional, linear-elastic, isotropic media. In the FEM, the element stiffness and mass matrices are defined by

$$\mathbf{K}^e = \int_{\Omega^e} \mathbf{B}^T \mathbf{D}\, \mathbf{B}\, d\Omega, \quad \mathbf{M}^e = \int_{\Omega^e} \mathbf{N}^T \rho\, \mathbf{N}\, d\Omega, \tag{1}$$

in which $\mathbf{B}$ and $\mathbf{N}$ are the strain-displacement and shape function matrices, $\mathbf{D}$ is the elasticity matrix, and ρ is the material density. Numerical integration is performed via Gaussian quadrature. The global dynamic stiffness matrix used in harmonic analysis is given by

$$\mathbf{K}^s = \mathbf{K}_g - \omega^2 \mathbf{M}_g, \tag{2}$$

in which $\mathbf{K}_g$ and $\mathbf{M}_g$ are the assembled global stiffness and mass matrices.

2.2 Perfectly Matched Layer (PML)

To simulate unbounded domains and avoid artificial wave reflections at the boundaries of the FEM domain used to describe the soil in this paper, the Perfectly Matched Layer is employed. This is achieved by introducing a complex coordinate transformation into the governing elastodynamic equations. The transformation replaces the physical coordinates x_i by stretched coordinates $\tilde{x}_i$, defined as

$$\tilde{x}_i = \int_0^{x_i} \lambda_i(\xi)\, d\xi, \tag{3}$$

in which $\lambda_i(x_i)$ is a nonzero complex-valued stretching function. This transformation implies the following relation between partial derivatives:

$$\frac{\partial}{\partial \tilde{x}_i} = \frac{1}{\lambda_i(x_i)} \frac{\partial}{\partial x_i}. \tag{4}$$

Substituting this relation into the standard elastodynamic equations leads to the modified set of equations governing wave propagation in the PML (Josifovski, 2016):

$$\frac{1}{\lambda_j(x_j)} \frac{\partial \sigma_{ij}}{\partial x_j} = -\omega^2 \rho u_i, \qquad \sigma_{ij} = C_{ijkl}\, \varepsilon_{kl}, \qquad \varepsilon_{ij} = \frac{1}{2}\left(\frac{1}{\lambda_j(x_j)} \frac{\partial u_i}{\partial x_j} + \frac{1}{\lambda_i(x_i)} \frac{\partial u_j}{\partial x_i} \right). \tag{5}$$

The stretching function $\lambda_j(x_j)$ is expressed as (Fontara *et al.*, 2017)

$$\lambda_i(x_i) = 1 + \left[\frac{f_i(x_i)}{a_0^*} \right] - i \frac{f_i(x_i)}{a_0^*}, \quad f_i(x_i) = f_0 \left(\frac{x_i}{L_p} \right)^m, \tag{6}$$

in which $a_0^* = \omega T_{PML}/c_s$ is the dimensionless frequency, T_{PML} is the thickness of the PML layer, c_s is the shear wave velocity, and ω is the angular frequency of the incident wave, f_0 is the amplitude, and m is the polynomial order of the function.

3. NUMERICAL RESULTS

In this section, numerical simulations are presented to evaluate the influence of surface and partially buried structures on ground vibration attenuation. The effectiveness of the PML formulation is assessed by reproducing benchmark cases from the literature. Once verified, the model is used to analyze the problem of partially buried walls as ground vibration attenuators.

3.1 Verification

To verify the FEM implementation and the PML formulation, classical reference cases were modeled in COMSOL MULTIPHYSICS® software, adopting 2D axisymmetric domains when symmetry was present. The structures and soil are fully discretized using the FEM, and a PML of thickness T_{PML} is added to the domain boundaries to suppress spurious reflections.

3.1.1 Surface Plate and Piled Foundation

The first verification problem consists of a rigid plate on the soil surface supported by a single embedded pile, as shown in Fig. 2. The reference solution of this problem has been presented by Barros *et al.* (2019), and solved using the Boundary Element Method. A vertical harmonic excitation is applied at the center of the plate, and the response of the piled plate system is measured according to the normalized vertical compliance

$$c_z^* = \frac{c_{zz}}{c_{zz}(a_0^* = 0)}, \quad \text{with} \quad c_{zz} = \frac{u_0 a_b \mu_s}{F}, \tag{7}$$

in which u_0 is the vertical displacement, a_b is the plate radius, and F is the excitation amplitude.

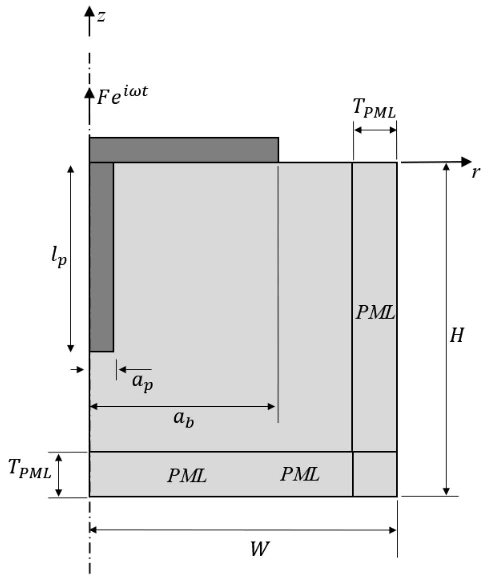

Figure 2: Surface plate with embedded pile.

The results are expressed in terms of the normalized excitation frequency

$$a_0^* = \frac{\omega \cdot a_b}{c_s}, \quad \text{in which} \quad c_s = \sqrt{\frac{\mu_s}{\rho_s}}, \tag{8}$$

is the shear wave velocity of the soil, and μ_s is the Lamé constant of the soil. The plate is assumed to be rigid and massless, with stiffness 1000 times higher than the soil. Fig. 3 shows good agreement with the reference results, verifying the modeling approach.

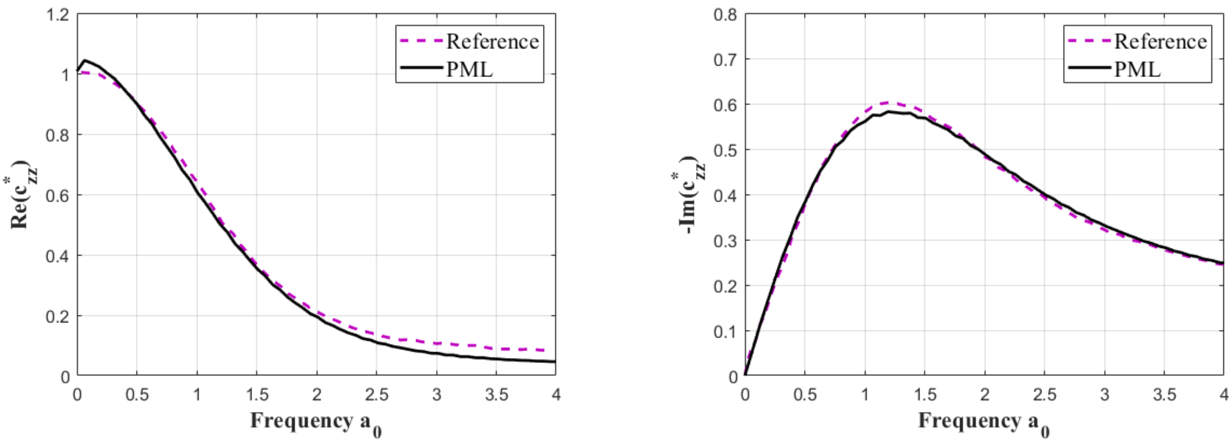

(a) Real part

(b) Imaginary part

Figure 3: Comparison of the response of a rigid surface plate subjected to external excitation.

The response of the embedded pile is further evaluated using the vertical impedance in terms of the normalized excitation frequency a_0, given by

$$K_{zz} = \frac{F}{u_0 \omega \mu_s} \quad \text{and} \quad a_0 = \frac{\omega \cdot a_p}{c_s} \tag{9}$$

with parameters $l_p = 12a_p$, $a_b = 12a_p$, $E_p = 1000E_s$, $\rho_p = 2\rho_s$, and $\nu_s = 0.25$. The results in Fig. 4 show a good agreement of the present PML approach with the reference solution.

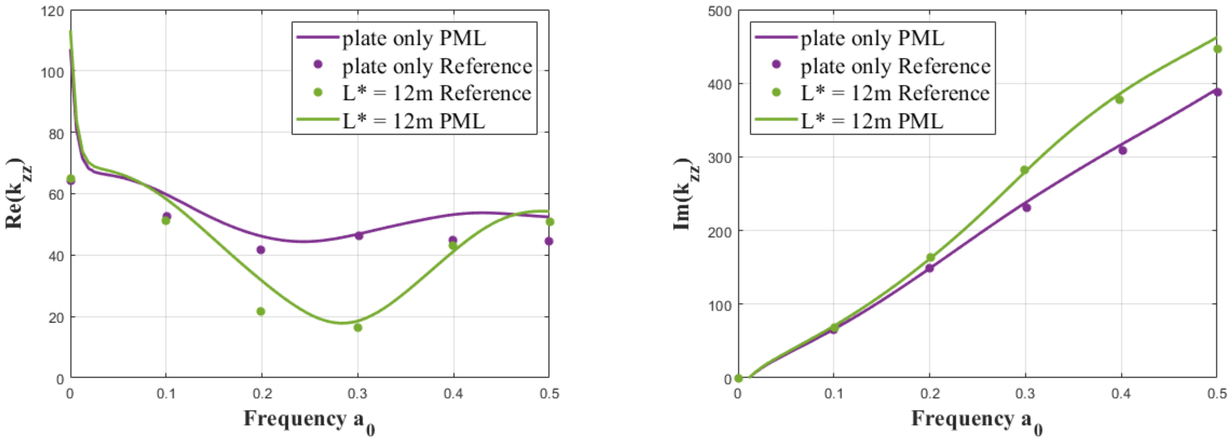

(a) Real part (b) Imaginary part

Figure 4: Comparison of vertical stiffness of piled plate.

3.1.2 Surface Walls

The second verification case considers the problem of surface walls (Fig. 5) studied by Carneiro *et al.* (2022). The dynamic response is quantified by insertion loss

$$\mathrm{IL} = 20\log_{10}\left(\frac{u_b}{u_a}\right) \tag{10}$$

in which u_b and u_a are the displacements with and without the wall, respectively. The material properties considered in this problem are shown in Table 1.

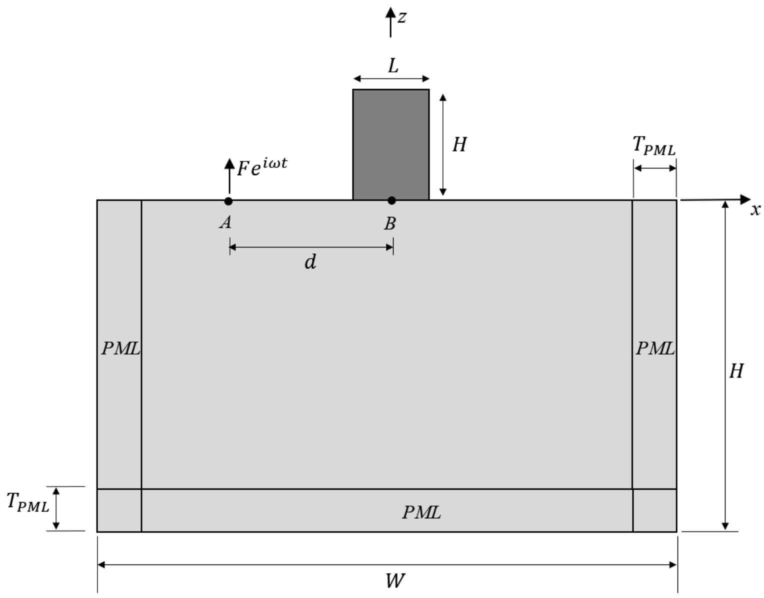

Figure 5: Surface wall.

Table 1: Materials Parameters

Material	Young's Modulus [MPa]	Poisson's Ratio	Density [kg/m³]	Damping
Soil	361	0,485	1945	0.025
Wall	367	0,2	1700	0.02

Figure 6 shows the IL at the point in which the wall is installed ($x = 0$), due to a load applied at $d = 5$m, which is consistent with the reference Carneiro *et al.* (2022).

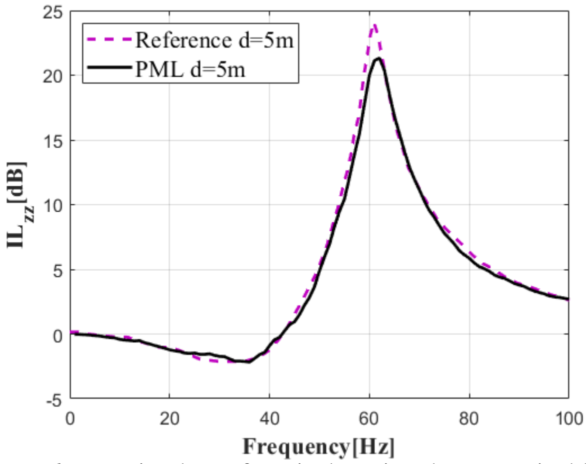

Figure 6: Insertion loss of vertical motion due to vertical loads.

3.2 Multiple Walls

Once verified with the cases above, the model was extended to analyze the case of a series of walls on the soil surface. The results consider the cases of two and five walls spaced by 1m from each other, center-to-center (Fig. 7). The excitation is placed 5m to the left of the leftmost wall, and the insertion loss IL is computed at point B, 20m to the right of the rightmost wall. Figure 8 shows that including more walls on the soil surface results in increased vibration attenuation performance of the system, for the set of results considered.

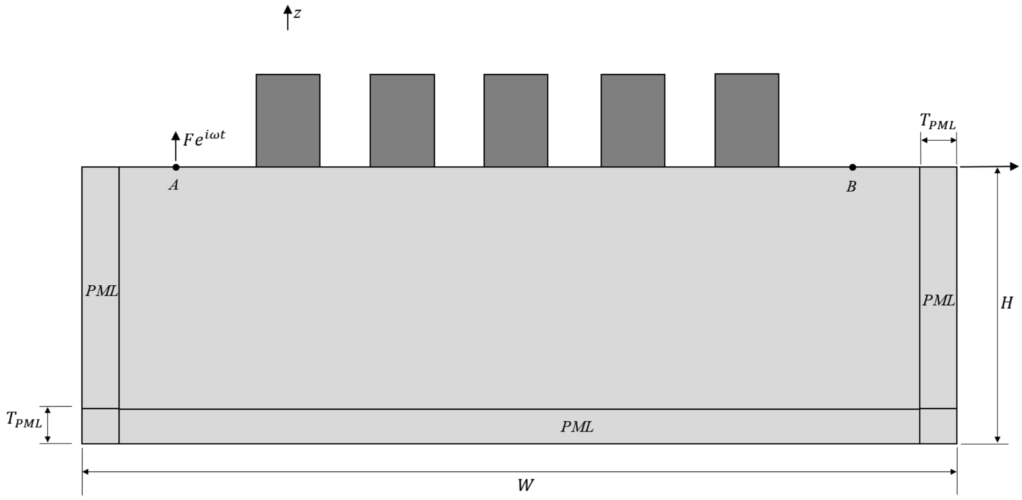

Figure 7: Schematic of the updated layout featuring multiple walls.

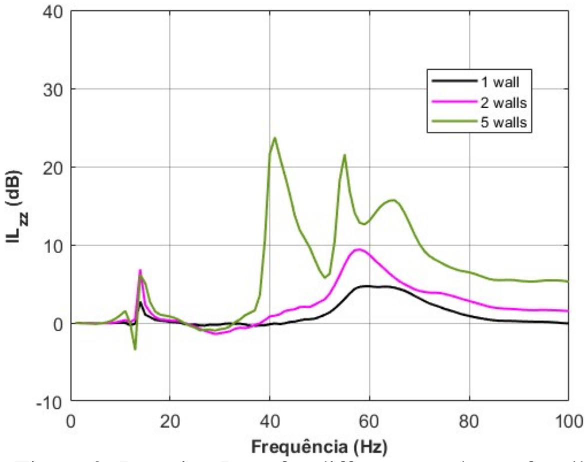

Figure 8: Insertion Loss for different numbers of walls.

3.3 Partially Buried Walls

To explore the influence of wall embedment in its vibration attenuation performance, this section considers the case of a single wall buried at varying depths H_s (Fig. 1). Figure 9 shows that increasing the depth of embedment of the wall has no direct correlation with its attenuation performance. Although all cases promote vibration attenuation in most of the frequency spectrum, each embedment case yields different performances in different parts of the spectrum. The most appropriate embedment must be selected for each wall based on the specific frequency of excitation.

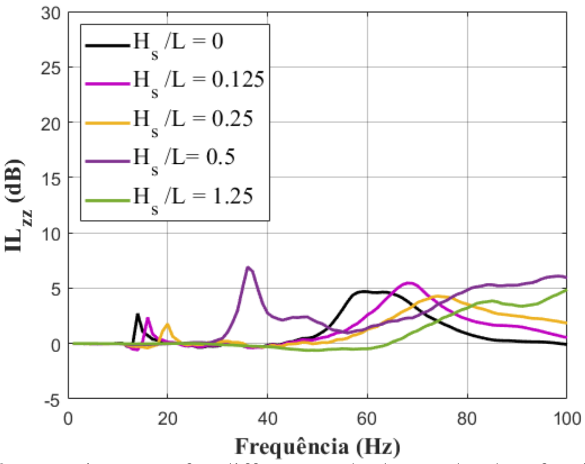

Figure 9: Insertion Loss for different embedment depths of a single wall.

4. CONCLUSION

This study presented a numerical framework based on the FEM together with the PML to analyze ground vibration attenuation promoted by series of surface walls and by partially buried walls. The model was verified against benchmark cases from the literature, demonstrating agreement. These results confirm that the use of PML effectively suppresses boundary reflections, enabling accurate simulation of unbounded elastic domains. Simulations with surface walls showed that increasing the number of barriers enhances attenuation, while analyses with partially buried walls showed that the appropriate depth of embedment must be selected in each application. Overall, the proposed approach provides a reliable and flexible tool for investigating soil–structure interaction and designing efficient vibration mitigation strategies.

5. ACKNOWLEDGEMENTS

The research leading to this paper has been funded in part by the São Paulo Research Foundation (Fapesp) through grant 2022/02753-5.

6. REFERENCES

Barros, P.L., Labaki, J. and Mesquita, E., 2019. "Ibem-fem model of a piled plate within a transversely isotropic half-space". *Engineering Analysis with Boundary Elements*, Vol. 101, pp. 281–296.

Baziar, M.H. and Shahbazan, P., 2024. "Centrifuge modeling of heavy masses, placed on the ground, as a vibration attenuation countermeasure for surface trains". *Transportation Geotechnics*, Vol. 45, p. 101196.

Carneiro, D., Barros, P.L. and Labaki, J., 2022. "Ground vibration attenuation performance of surface walls". *Computers and Geotechnics*, Vol. 149, p. 104715.

Dijckmans, A., Coulier, P., Jiang, J., Toward, M., Thompson, D., Degrande, G. and Lombaert, G., 2015. "Mitigation of railway induced ground vibration by heavy masses next to the track". *Soil Dynamics and Earthquake Engineering*, Vol. 75, pp. 158–170.

Fontara, I.K., Schepers, W., Savidis, S. and Rackwitza, F., 2017. "Fe/pml numerical schemes for dynamic soil-structure interaction and seismic wave propagation analysis". *Procedia Engineering*, Vol. 199, pp. 2348–2353.

Jiang, Y., Meng, F., Chen, Y., Zheng, Y., Chen, X., Zhang, J. and Huang, X., 2020. "Vibration attenuation analysis of periodic underground barriers using complex band diagrams". *Computers and Geotechnics*, Vol. 128, p. 103821.

Josifovski, J., 2016. "Analysis of wave propagation and soil–structure interaction using a perfectly matched layer model". *Soil Dynamics and Earthquake Engineering*, Vol. 81, pp. 1–13.

Li, Z., Ma, M., Liu, K. and Jiang, B., 2023. "Performance of rubber-concrete composite periodic barriers applied in attenuating ground vibrations induced by metro trains". *Engineering Structures*, Vol. 285, p. 116027.

Moghadam, A.E. and Rafiee-Dehkharghani, R., 2022. "Ground-borne vibration screening in layered dry and saturated grounds using optimal inclined wave barriers". *Soil Dynamics and Earthquake Engineering*, Vol. 162, p. 107448.

Pu, X., Shi, Z. and Xiang, H., 2018. "Feasibility of ambient vibration screening by periodic geofoam-filled trenches". *Soil Dynamics and Earthquake Engineering*, Vol. 104, pp. 228–235.

Tsai, P.h., Feng, Z.y. and Jen, T.l., 2008. "Three-dimensional analysis of the screening effectiveness of hollow pile barriers for foundation-induced vertical vibration". *Computers and Geotechnics*, Vol. 35, No. 3, pp. 489–499.

7. RESPONSIBILITY NOTICE

The authors are solely responsible for the printed material included in this paper.